frontiers | Frontiers in Environmental Chemistry

ORIGINAL RESEARCH
published: 25 August 2022
doi: 10.3389/fenvc.2022.898879

Photocatalytic Activity of Zero-Valent Iron Nanoparticles Highly Dispersed on Porous Carbon Materials

Dan Liang[1†], Yanfei Fan[1†], Taixing Yue[2], Wen Wang[1], Qiaoyan Shang[1], Ping Chen[1], Minghui Zhu[1], Yan Liu[1], Guanwei Cui[1] and Bo Tang[1]*

[1]College of Chemistry, Chemical Engineering and Materials Science, Shandong Normal University, Jinan, China, [2]Shandong Provincial Eco-environment Monitoring Center, Jinan, China

During the traditional homogeneous Fenton reaction process for water treatment, the consumption rate constant of Fe^{2+} is much greater than its regeneration rate constant, which makes Fe^{2+} an almost stoichiometric loss and produces iron sludge waste. In this article, highly dispersed zero-valent Fe nanoparticles loaded on porous carbon materials (Fe-EMC) were synthesized by a one-step calcination method using *Flammulina velutipes* natural carbon source and $Fe(NO_3)_3$ as raw materials to solve the aforementioned problem. The as-prepared Fe-EMC materials are characterized by X-ray diffraction analysis, scanning electron microscopy, electron probe microanalyzer, high-resolution transmission electron microscopy, X-ray photoelectron spectroscopy, and N_2 adsorption–desorption measurements. It exhibits excellent photocatalytic activity for the degradation of methylene blue (MB) dyes under a broad pH region. Under conditions of 0.3 g/L Fe-EMC, 0.2 M/L H_2O_2, pH 7.0–11.0, and 50 mg/L MB, 97.98% of the MB dyes in the solution were completely degraded within 1 h. It was attributed to the efficient regeneration cycle between Fe^{2+} and Fe^{3+} in the Fenton-like system with light irradiation, which can promote the generation of active oxygen species.

Keywords: zero-valent iron, photocatalytic degradation, Flammulina velutipes, carbon, Fenton-like system

OPEN ACCESS

Edited by:
Ahmed El Nemr, National Institute of Oceanography and Fisheries (NIOF), Egypt

Reviewed by:
Chongqing Wang, Zhengzhou University, China
Teza Mwamulima, The University of Melbourne, Australia

****Correspondence:***
Guanwei Cui
cuiguanwei@sdnu.edu.cn

†These authors have contributed equally to this work and share first authorship

Specialty section:
This article was submitted to Catalytic Remediation, a section of the journal Frontiers in Environmental Chemistry

Received: *01 April 2022*
Accepted: *10 June 2022*
Published: *25 August 2022*

Citation:
Liang D, Fan Y, Yue T, Wang W, Shang Q, Chen P, Zhu M, Liu Y, Cui G and Tang B (2022) Photocatalytic Activity of Zero-Valent Iron Nanoparticles Highly Dispersed on Porous Carbon Materials. Front. Environ. Chem. 3:898879. doi: 10.3389/fenvc.2022.898879

INTRODUCTION

The Fenton reaction is a kind of advanced oxidation process for the degradation of organic pollutants. It is based on the addition of H_2O_2 to the wastewater or leachate in the presence of ferrous salts as catalysts to produce strong oxidizing active oxygen·OH which can decompose organic pollutants into H_2O and CO_2 (Lyu and Hu, 2017; Zhu et al., 2019). Due to advantages such as mild reaction conditions, fast reaction speed, strong oxidation capacity, and high removal efficiency, the Fenton reaction has been widely applied in wastewater treatment. However, the·OH concentration produced in the Fenton reaction is severely affected by the material ratio and can only be effectively performed under acidic conditions. Moreover, during the traditional homogeneous Fenton reaction process, iron ions undergo a complex catalytic cycle between divalent iron ions and trivalent iron ions. Several studies have shown that the consumption rate constant of Fe^{2+} is much greater than its regeneration rate constant (Umar et al., 2010), which makes it difficult for the traditional Fenton reaction to cycle efficiently (Liang et al., 2021). Therefore, Fe^{2+} is almost stoichiometrically lost and not the way it has been interpreted, which results in producing iron sludge waste that absorbs a large amount of organic pollutants or degrades intermediate substances, which may lead to secondary environmental pollution (Bokare and Choi, 2014). Due to this reason, overcoming the

aforementioned shortcomings has become a research hotspot in recent years. Some studies have shown that the introduction of auxiliary means of illumination in the traditional Fenton treatment process can improve the catalytic cycle between Fe^{3+} and Fe^{2+}, thereby increasing the production of·OH which can improve the degradation efficiency of the Fenton system (Wai et al., 2003; Zhu et al., 2019; Zhu et al., 2021).

In recent years, researchers have found that the combination of zero-valent iron (ZVI), O_2, H_2O_2, and other oxidants can form a Fenton-like system to generate hydroxyl radicals (Mylon et al., 2010), resulting in high efficiency of organic pollutants' degradation (Stieber et al., 2011). This method, to a certain extent, overcomes the aforementioned shortcomings of the traditional Fenton reaction and can even effectively remove heavy metals while removing organic pollutants (O'carroll et al., 2013). In particular, nanoscale zero-valent iron particles are highly reactive due to their specific surface area; surface effects; quantum size effects; and special optical, electrical, and magnetic properties (Ryu et al., 2011). However, due to their high surface energy, iron nanoparticles tend to agglomerate during synthesis and application (Jiang et al., 2014).

Loading on bulk materials is an effective way to avoid the agglomeration of nanoparticles (Liu, 2017), and carbon materials are often used as supporting materials for metal catalysts (Guo et al., 2015; Han et al., 2017). Especially in the wastewater treatment process, porous carbon carriers with strong adsorption capacity can also enrich pollutants and improve the pollutant removal efficiency (Liu and Gao, 2004). Wang et al. (2020) constructed a series of superior Fenton-like catalytic systems with zero-valent iron or iron oxides loaded on different carbon materials derived from microplastics and biomass, such as tea leaves and sawdust, and they have been successfully applied to the degradation or decolorization of organic pollutants such as antibiotics and dyes in wastewater (Wang et al., 2021a; Wang et al., 2021b; Wang et al., 2022). In this article, inspired by previous works, a Fenton-like catalytic system was constructed by combining zero-valent iron loading and photo-assisted methods to solve the aforementioned iron catalytic cycle and iron nanoparticle aggregation problems. In view of the characteristics of rapid growth, diverse element composition, and rich pore structure of *Flammulina velutipes*, it was used as the biomass carbon carrier of zero valent iron. Highly dispersed Fe nanoparticles loaded on porous carbon materials (Fe-EMC) were prepared by calcining the mixture of *Flammulina velutipes* and iron nitrate. The as-prepared Fe-EMC photocatalyst was applied in the photo-Fenton process to degrade methylene blue (MB) dye, which can overcome the aforementioned limitations of the homogeneous photo-Fenton process to a certain extent.

EXPERIMENT

Materials and Instruments

$Fe(NO_3)_3{\cdot}9H_2O$, H_2O_2, p-Phthalic acid (TAOH), tert-butyl alcohol (TBA), and MB dyes were purchased from Shanghai Macklin Biochemical Co., Ltd. All the chemicals were of AR grade. *Flammulina velutipes* were purchased from the supermarket. The ultrapure water used in the experiment was Wahaha pure water.

The morphologies of the as-obtained product were characterized using a scanning electron microscope (SEM) equipped with a field-emission gun operated at 5.0 kV. The element distribution in the catalysts was analyzed by energy-dispersive spectroscopy (EDS) using Hitachi's SU8010 instrument made in Japan. High-resolution transmission electron microscopy (HRTEM) was taken on a JEM-2100F instrument at an accelerating voltage of 200 kV. X-ray diffraction (XRD) analysis was carried out on a Bruker D8 Advance diffractometer with Cu Kα radiation (1.5418 Å). X-ray photoelectron spectroscopy (XPS) was conducted on a Thermo Scientific Escalab 250 Xi with Al Kα as the excitation source. The pore size of the catalysts was analyzed by Brunner–Emmet–Teller (BET) and measured with an ASAP 2020 PLU HD88 instrument manufactured by Shanghai Micromeritics Instrument Co., Ltd.

Synthesis of Fe-EMC

Flammulina velutipes were cut into pieces and soaked in 0.5 mol/L iron nitrate solution for 24 h. Then, it was taken out and dried in the oven at 120°C for 5 h. The dried *Flammulina velutipes* were calcined at 800°C for 3 h in a N_2 atmosphere. Finally, a black irregular granular Fe-EMC catalyst was obtained. The synthesis process of Fe-EMC is shown in **Figure 1**.

Photocatalytic Activity of MB Dyes Degradation

The photocatalytic activity test for MB dye degradation was performed on an XPA-7 photocatalytic reaction instrument. In a typical process, 12.0 mg of photocatalyst was dispersed with 40.0 ml of MB dye solution in a 60-ml quartz tube. The sample solution was stirred for 8 h to reach adsorption equilibrium (**Supplementary Figure S1**). Then, it was irradiated with a 1000-W Xe lamp at room temperature with constant stirring. After that, sampling was performed at regular intervals within a fixed period of time. After removing the catalyst with a filter membrane, the absorption spectrum was measured with an ultraviolet-visible spectrophotometer, and the mineralization rate was measured with a chemical oxygen demand (COD) meter.

RESULTS AND DISCUSSION

Morphology and Structure of Fe-EMC

The particle sizes of the as-prepared Fe-EMC photocatalyst range from one micron to tens of microns (**Figure 2A**). Bundle tubular structures were observed from the cross-section of particles, which may have originated from the pristine structure of *Flammulina velutipes* (**Supplementary Figure S2**). The N_2 adsorption-desorption measurements show that the material has a mesoporous slit-type structure with a main pore size of 20 nm and a BET surface area of approximately 169.43 m^2g^{-1} (**Supplementary Figure S3**). From the HRTEM images

FIGURE 1 | Scheme of the synthesis process of Fe-EMC.

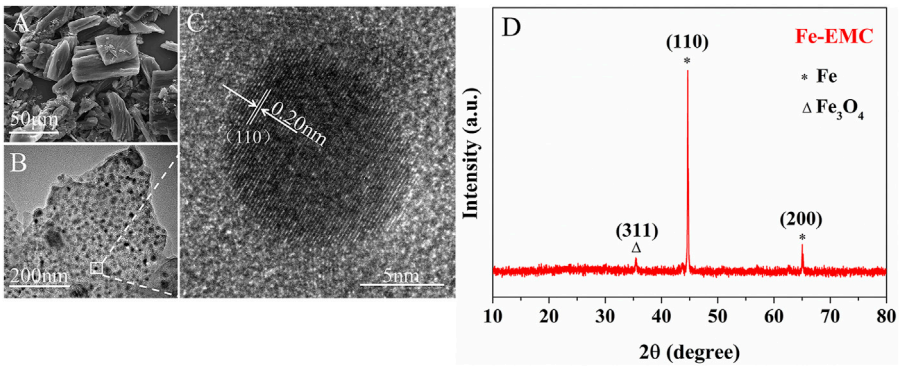

FIGURE 2 | Morphology and structure characterizations of Fe-EMC. **(A)** SEM; **(B,C)** HRTEM; **(D)** XRD.

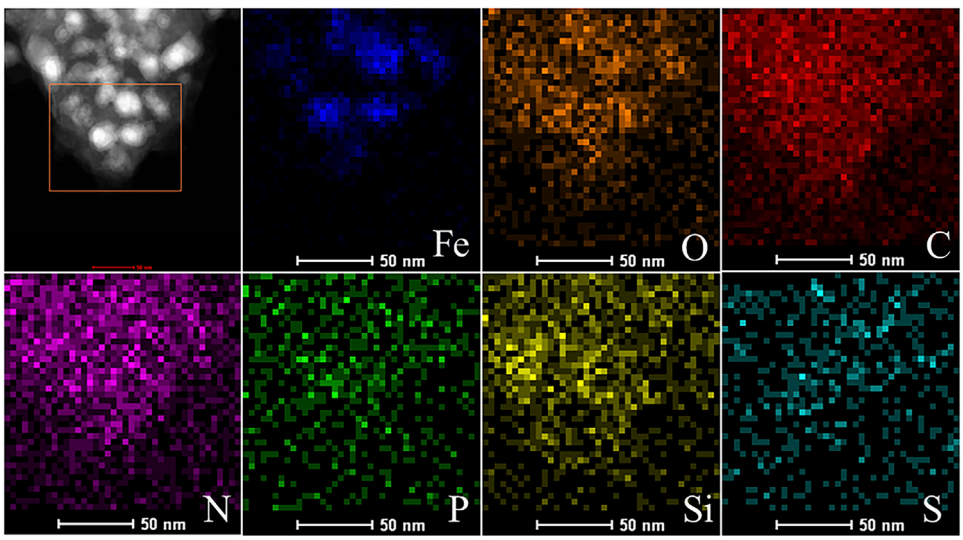

FIGURE 3 | EDS mapping images of Fe-EMC.

(**Figure 2B**), it can be observed that Fe nanoparticles with a size of 10 nm are loaded and well-distributed on the carbonized *Flammulina velutipes*. The lattice fringe with a size of 0.20 nm is consistent with the Fe (110) lattice fringe (**Figure 2C**).

The XRD peaks centered at 44.7° and 65.0° were ascribed to the (110) and (200) crystal planes of Fe, respectively (PDF#06-0696). A weak peak centered at 35.4° was ascribed to the (311) crystal plane of Fe_3O_4 (PDF#19-0629) (**Figure 2D**). For comparison, the decomposition products of $Fe(NO_3)_3$ calcined at 800°C without *Flammulina velutipes* is Fe_2O_3 (PDF#33-0664) (**Supplementary Figure S4**). It indicates that the $Fe(NO_3)_3$ was almost completely reduced by *Flammulina velutipes* under high temperature.

The distribution of Fe nanoparticles on the Fe-EMC was further determined by the EDS mapping images (**Figure 3**). In addition, a uniform distribution of C, N, O, P, Si, and S elements, all originating from the *Flammulina velutipes* carbon source, was

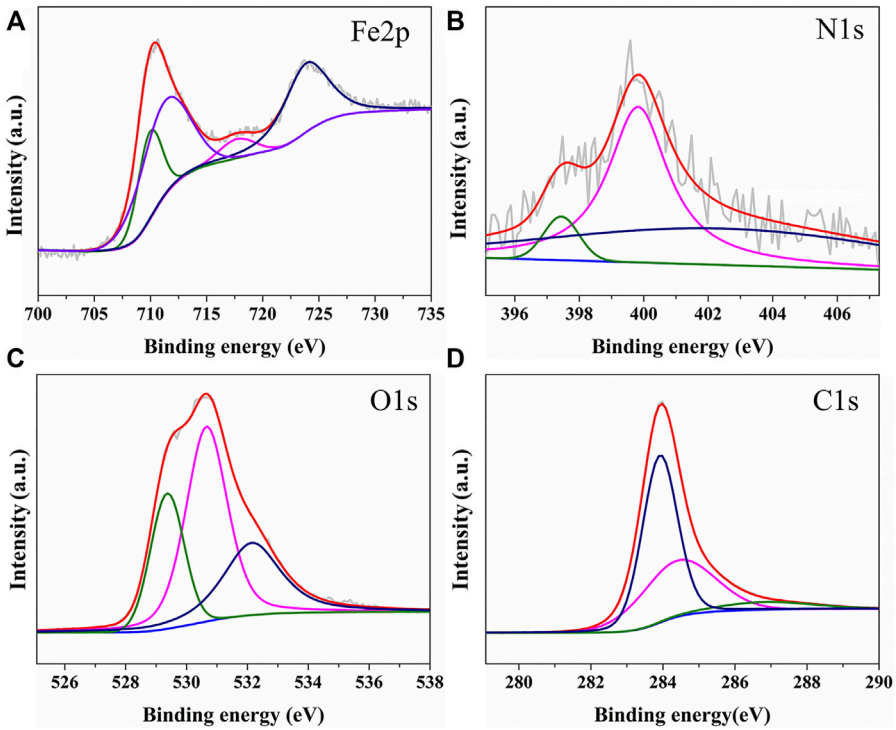

FIGURE 4 | XPS of Fe-EMC. **(A)** Fe2p; **(B)** N1s; **(C)** O1s; **(D)** C1s.

also observed on Fe-EMC. It can be concluded that the distribution state of O element is almost consistent with that of Fe element. This indicates that although iron oxides are clearly observed from the HRTEM images, some amorphous iron oxides might exist independently or on the surface of Fe nanoparticles, which was further confirmed by subsequent XPS results.

The chemical states of the surface species of Fe-EMC were determined by X-ray photoelectron spectroscopy (XPS) (**Supplementary Figure S5**; **Figure 4**). Consistent with the EDS-mapping test results, seven elements, including Fe, C, N, O, P, Si, and S, can be observed in the XPS spectrum (**Supplementary Figure S5**). Among them, four main elements (Fe, C, N, and O) have higher spectral peak intensities, and the four peaks of Fe2p are shown in **Figure 4A**. The XPS peaks centered at 709.93 eV were ascribed to element Fe^0 $2p_{3/2}$ (Mathieu and Landolt, 1986). The XPS peaks centered at 711.23 and 723.83 eV were ascribed to Fe^{3+} $2p_{3/2}$ and $Fe^{2+}2p_{1/2}$ of Fe_3O_4, respectively (Hidetaka and Masichi, 1980; Tan et al., 1990). The XPS peaks centered at 717.68 eV was ascribed to Fe $2p_{3/2}$ of non-stoichiometric Fe oxides (Daas et al., 1994). The three XPS peaks of N1s centered at 397.44, 399.13, and 402.51 eV were ascribed to metal nitrogen (Biwer and Bernasek, 1986), pyridine nitrogen (Barber et al., 1973), and graphene nitrogen (Baumgarten et al., 1996), respectively (**Figure 4B**). The three XPS peaks centered at 529.37, 530.66, and 532.15 eV were attributed to the O1s in iron oxides and carbon oxides (Tan et al., 1990; Lopez et al., 1991; Marcus and Grimal, 1992) (**Figure 4C**). The three XPS peaks of C1s centered at 283.92, 284.41, and 286.83 eV were ascribed to -C*H=CH- (Wu and Chen, 1988), C*-C (Morar et al., 1986), and C*-O (Castner and Ratner, 1990), respectively (**Figure 4D**).

Evaluation of Photocatalytic Activity of Fe-EMC

The photocatalytic activity of Fe-EMC was determined by the photocatalytic degradation of MB dyes. It was found that about 27.37% of the MB dye in the solution was adsorbed by Fe-EMC at the adsorption equilibrium point in darkness (**Supplementary Figure S1**). Under the optimal reaction conditions (**Supplementary Figure S6**), 97.98% of MB dye in solution was completely degraded within 1 h, which was determined by COD testing. Blank comparison experiments showed that light irradiation, catalyst, and hydrogen peroxide are the three necessary conditions for obtaining excellent photocatalytic performance (**Figure 5A**; **Supplementary Figure S7**). Furthermore, as shown in **Supplementary Figure S8**, unlike the traditional Fenton reaction, this Fenton-like photocatalytic system has a wide applicable pH range from 3 to 11 (**Supplementary Figure S8**). Because Fe-EMC has ferromagnetism, it can be easily separated and recovered by magnetic adsorption (**Supplementary Figure S9**). After five cycles, the catalytic activity of Fe-EMC did not decrease significantly (**Figure 5B**).

Mechanism Investigation

Herein, the excellent photocatalytic degradation efficiency of Fe-EMC photocatalysts is mainly due to the faster catalytic

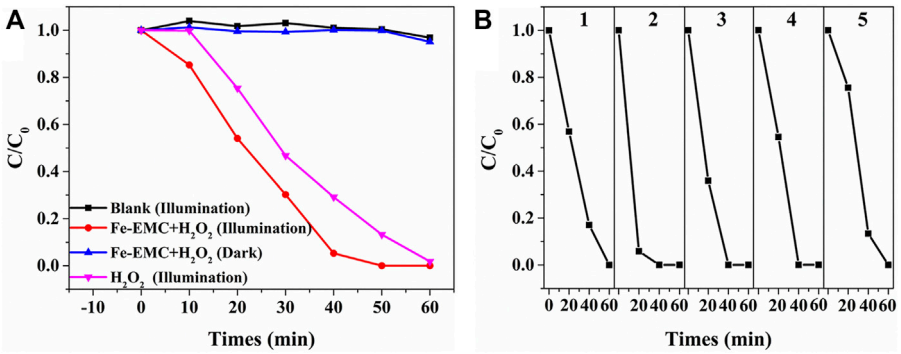

FIGURE 5 | (A) MB dye photocatalytic discoloration plots of Fe-EMC samples with H_2O_2 under different reaction conditions; **(B)** photocatalytic activity cycle tests of Fe-EMC samples under full-spectrum light irradiation. 0.3 g/L Fe-EMC, 0.2 mol/L H_2O_2, pH 7.0, and 50 mg/L MB at room temperature.

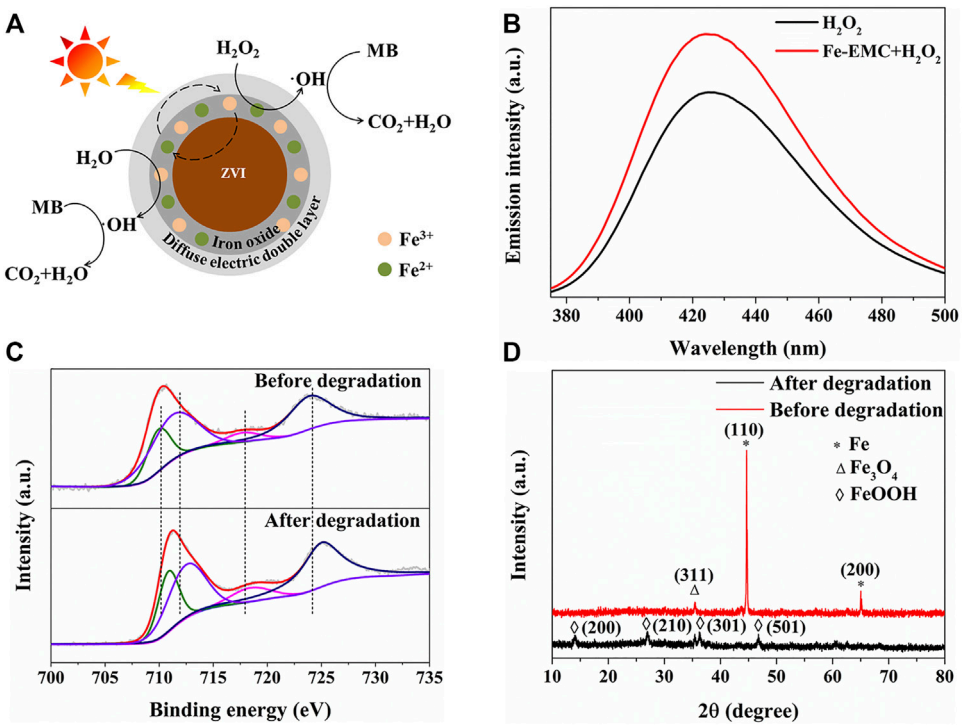

FIGURE 6 | (A) The reaction mechanism of the Fe-EMC photocatalytic system; **(B)** fluorescence spectrum of TAOH under different reaction conditions after 50 min of full-spectrum light irradiation, TAOH 5.0 mmol/L, 0.3 g/L Fe-EMC, 0.2 mol/L H_2O_2, pH 7.0, and 50 mg/L MB at room temperature; XPS spectra **(C)** and XRD patterns **(D)** of Fe-EMC before and after photocatalytic reaction.

regeneration cycle between Fe^{2+} and Fe^{3+} under light conditions, which will promote the generation of active oxygen·OH. As shown in **Figure 6A**, the Fe^{2+} present on the surface of Fe of the catalyst may be regenerated through two possible routes. The first route is that the generated Fe^{3+} interacts with internal zero-valent iron or other intermediate reducing agents such as HO_2 and $R^{\cdot}$ to regenerate Fe^{2+} (Liang et al., 2021). The second route is that iron oxides perform a typical semiconductor photocatalytic redox process to realize the regeneration of Fe^{2+} (Nguyen et al., 2017). During the aforementioned photocatalytic reaction process, light not only promotes the regeneration cycle of Fe^{2+}, but also plays a positive role in the production of reactive oxygen species, such as·OH, thereby improving the degradation efficiency of the Fenton reaction. As shown in **Figure 6B**, the intermediate·OH was determined by the fluorescence probe terephthalic acid (TA). It was found that the concentration of·OH in the Fe-EMC photocatalytic system increases more rapidly and higher than that of the typical Fenton

reaction. Moreover, MB degradation is significantly inhibited with the addition of TBA (**Supplementary Figure S10**). It indicated that OH played a key role during the photocatalytic degradation of MB dyes (Wang et al., 2021c). Both the XPS and XRD test results (**Figures 6C,D**) show that after five photocatalytic reaction cycles, the content of iron oxides, especially FeOOH (PDF#44-1415), increased significantly, while the photocatalytic efficiency did not decrease, which proved the aforementioned photocatalytic mechanism from the side. Previous studies have shown that light helps to dissociate·OOH from FeOOH formed during the Fenton reaction, resulting in improved degradation efficiency of the Fenton reaction (Nguyen et al., 2017).

CONCLUSION

In this article, a Fe-EMC photocatalyst was synthesized by a one-step calcination method using *Flammulina velutipes* natural carbon source and $Fe(NO_3)_3$ as raw materials. The as-prepared Fe-EMC photocatalyst has an excellent photocatalytic degradation effect on MB dyes. This is attributed to the efficient regeneration cycle between Fe^{2+} and Fe^{3+} under light conditions, which can promote the generation of active oxygen species. Moreover, unlike the traditional Fenton reaction, the proposed Fe-EMC photocatalytic system has a wide pH range and a long-life photocatalytic activity, indicating that the catalyst has strong applicability to actual wastewater treatment processes.

DATA AVAILABILITY STATEMENT

The raw data supporting the conclusion of this article will be made available by the authors, without undue reservation.

AUTHOR CONTRIBUTIONS

GC conceived and designed the experiments. DL, YF, WW, MZ, and YL performed the experiments. YF, TY, and QS analyzed the data. GC, DL, and PC co-wrote the paper. BT supervised the article.

FUNDING

This research was funded by the National Natural Science Foundation of China (21927811, 22076105, 21575082, 91753111, and 21976110) and the Key Research and Development Program of Shandong Province (2018YFJH0502), Development plan of science and technology for Shandong Province of China (2013GGX10706), and A Project of Shandong Province Higher Educational Science and Technology Program (J13LD06).

SUPPLEMENTARY MATERIAL

The Supplementary Material for this article can be found online at: https://www.frontiersin.org/articles/10.3389/fenvc.2022.898879/full#supplementary-material

REFERENCES

Barber, M., Connor, J. A., Guest, M. F., Hillier, I. H., Schwarz, M., and Stacey, M. (1973). Bonding in Some Donor-Acceptor Complexes Involving Boron Trifluoride. Study by Means of ESCA and Molecular Orbital Calculations. *J. Chem. Soc. Faraday Trans. 2* 69, 551–558. doi:10.1039/f29736900551

Baumgarten, E., Fiebes, A., Stumpe, A., Ronkel, F., and Schultze, J. W. (1996). Synthesis and Characterization of a New Platinum Supported Catalyst Based on Poly-{acrylamide-Co-[3-(acryloylamino)propyltrimethylammoniumchloride]} as Carrier. *J. Mol. Catal. A Chem.* 113, 469–477. doi:10.1016/S1381-1169(96)00275-0

Biwer, B. M., and Bernasek, S. L. (1986). Electron Spectroscopic Study of the Iron Surface and its Interaction with Oxygen and Nitrogen. *J. Electron Spectrosc. Relat. Phenom.* 40, 339–351. doi:10.1016/0368-2048(86)80044-5

Bokare, A. D., and Choi, W. (2014). Review of Iron-free Fenton-like Systems for Activating H2O2 in Advanced Oxidation Processes. *J. Hazard. Mater.* 275, 121–135. doi:10.1016/j.jhazmat.2014.04.054

Castner, D. G., and Ratner, B. D. (1990). Surface Characterization of Butyl Methacrylate Polymers by XPS and Static SIMS. *Surf. Interface Anal.* 15, 479–486. doi:10.1002/sia.740150807

den Daas, H., Passacantando, M., Lozzi, L., Santucci, S., and Picozzi, P. (1994). The Interaction of Cu(100)-Fe Surfaces with Oxygen Studied by X-Ray Photoelectron Spectroscopy. *Surf. Sci.* 317, 295–302. doi:10.1016/0039-6028(94)90285-2

Guo, C., Liao, W., Li, Z., Sun, L., and Chen, C. (2015). Easy Conversion of Protein-Rich Enoki Mushroom Biomass to a Nitrogen-Doped Carbon Nanomaterial as a Promising Metal-free Catalyst for Oxygen Reduction Reaction. *Nanoscale* 7, 15990–15998. doi:10.1039/c5nr03828f

Han, W., Li, Z., Li, Y., Fan, X., Zhang, F., Zhang, G., et al. (2017). The Promoting Role of Different Carbon Allotropes Cocatalysts for Semiconductors in Photocatalytic Energy Generation and Pollutants Degradation. *Front. Chem.* 5, 1–16. doi:10.3389/fchem.2017.00084

Hidetaka, K., and Masichi, N. (1980). X-ray Photoelectron Spectra of Hexavalentiton. *J. Electron Spectrosc. Relat. Phenom.* 18, 341–343. doi:10.1016/0368-2048(80)80021-1

Jiang, F., Li, X., Zhu, Y., and Tang, Z. (2014). Synthesis and Magnetic Characterizations of Uniform Iron Oxide Nanoparticles. *Phys. B Condens. Matter* 443, 1–5. doi:10.1016/j.physb.2014.03.009

Kwan, W. P., Voelker, B. M., and Bettina, M. (2003). Rates of Hydroxyl Radical Generation and Organic Compound Oxidation in Mineral-Catalyzed Fenton-like Systems. *Environ. Sci. Technol.* 37, 1150–1158. doi:10.1021/es020874g

Liang, W., Zhou, N. Q., Dai, C. M., Duan, Y. P., and Tu, Y. J. (2021). Research Progress of Organic Compounds Degradation by Fenton-Like System Based on Zero-Valent Iron. *Ag* 11, 426–434. doi:10.12677/ag.2021.114037

Liu, H.-t., and Gao, Y. (2004). Photocatalytic Decomposition of Phenol over a Novel Kind of Loaded Photocatalyst of TiO2/activated Carbon/silicon Rubber Film. *React. Kinet. Catal. Lett.* 83, 213–219. doi:10.1023/B:REAC.0000046079.56445.1f

Liu, Z. C. (2017). Reason for Aggregation of Nanoparticles in Nano-Materials and Solutions. *Value Eng.* 36, 157–158. doi:10.14018/j.cnki.cn13-1085/n.2017.13.065

López, G. P., Castner, D. G., and Ratner, B. D. (1991). XPS O 1s Binding Energies for Polymers Containing Hydroxyl, Ether, Ketone and Ester Groups. *Surf. Interface Anal.* 17, 267–272. doi:10.1002/sia.740170508

Lyu, L., and Hu, C. (2017). Heterogeneous Fenton Catalytic Water Treatment Technology and Mechanism. *Prog. Chem.* 29, 981–999. doi:10.7536/PC170552

Marcus, P., and Grimal, J. M. (1992). The Anodic Dissolution and Passivation of NiCrFe Alloys Studied by ESCA. *Corros. Sci.* 33, 805–814. doi:10.1016/0010-938X(92)90113-H

Mathieu, H. J., and Landolt, D. (1986). An Investigation of Thin Oxide Films Thermally Grown *In Situ* on Fe-24Cr and Fe-24Cr-11Mo by Auger Electron

Spectroscopy and X-Ray Photoelectron Spectroscopy. *Corros. Sci.* 26, 547–559. doi:10.1016/0010-938X(86)90022-3

Morar, J. F., Himpsel, F. J., Hollinger, G., Jordan, J. L., Hughes, G., and McFeely, F. R. (1986). C 1sexcitation Studies of Diamond (111). I. Surface Core Levels. *Phys. Rev. B* 33, 1340–1345. doi:10.1103/PhysRevB.33.1340

Mylon, S. E., Sun, Q., and Waite, T. D. (2010). Process Optimization in Use of Zero Valent Iron Nanoparticles for Oxidative Transformations. *Chemosphere* 81, 127–131. doi:10.1016/j.chemosphere.2010.06.045

Nguyen, X. S., Ji, W. D., and Li, J. (2017). Metal Doped Magnetite Based Magnetically Recoverable Catalysts for the Photo-Fenton Degradation of Organic Pollutants. *Build. Mat. World.* 38, 85–91. doi:10.3963/j.issn.1674-6066.2017.03.021

O'Carroll, D., Sleep, B., Krol, M., Boparai, H., and Kocur, C. (2013). Nanoscale Zero Valent Iron and Bimetallic Particles for Contaminated Site Remediation. *Adv. Water Resour.* 51, 104–122. doi:10.1016/j.advwatres.2012.02.005

Ryu, A., Jeong, S.-W., Jang, A., and Choi, H. (2011). Reduction of Highly Concentrated Nitrate Using Nanoscale Zero-Valent Iron: Effects of Aggregation and Catalyst on Reactivity. *Appl. Catal. B Environ.* 105, 128–135. doi:10.1016/j.apcatb.2011.04.002

Stieber, M., Putschew, A., and Jekel, M. (2011). Treatment of Pharmaceuticals and Diagnostic Agents Using Zero-Valent Iron - Kinetic Studies and Assessment of Transformation Products Assay. *Environ. Sci. Technol.* 45, 4944–4950. doi:10.1021/es200034j

Tan, B. J., Klabunde, K. J., and Sherwood, P. M. A. (1990). X-ray Photoelectron Spectroscopy Studies of Solvated Metal Atom Dispersed Catalysts. Monometallic Iron and Bimetallic Iron-Cobalt Particles on Alumina. *Chem. Mat.* 2, 186–191. doi:10.1021/cm00008a021

Umar, M., Aziz, H. A., and Yusoff, M. S. (2010). Trends in the Use of Fenton, Electro-Fenton and Photo-Fenton for the Treatment of Landfill Leachate. *Waste Manag.* 30, 2113–2121. doi:10.1016/j.wasman.2010.07.003

Wang, C., Huang, R., and Sun, R. (2020). Green One-Spot Synthesis of Hydrochar Supported Zero-Valent Iron for Heterogeneous Fenton-like Discoloration of Dyes at Neutral pH. *J. Mol. Liq.* 320, 114421. doi:10.1016/j.molliq.2020.114421

Wang, C., Huang, R., and Sun, R. (2022). Microplastics Separation and Subsequent Carbonization: Synthesis, Characterization, and Catalytic Performance of Iron/carbon Nanocomposite. *J. Clean. Prod.* 330, 129901. doi:10.1016/j.jclepro.2021.129901

Wang, C., Sun, R., Huang, R., and Cao, Y. (2021c). A Novel Strategy for Enhancing Heterogeneous Fenton Degradation of Dye Wastewater Using Natural Pyrite: Kinetics and Mechanism. *Chemosphere* 272, 129883–129889. doi:10.1016/j.chemosphere.2021.129883

Wang, C., Sun, R., and Huang, R. (2021a). Highly Dispersed Iron-Doped Biochar Derived from Sawdust for Fenton-like Degradation of Toxic Dyes. *J. Clean. Prod.* 297, 126681. doi:10.1016/j.jclepro.2021.126681

Wang, C., Sun, R., Huang, R., and Wang, H. (2021b). Superior Fenton-like Degradation of Tetracycline by Iron Loaded Graphitic Carbon Derived from Microplastics: Synthesis, Catalytic Performance, and Mechanism. *Sep. Purif. Technol.* 270, 118773. doi:10.1016/j.seppur.2021.118773

Wu, H.-M., and Chen, S.-A. (1988). Dopant-polymer Interaction: MoCl5-Doped Polyacetylene. *Synth. Met.* 26, 225–236. doi:10.1016/0379-6779(88)90239-1

Zhu, J., Zhang, G., Xian, G., Zhang, N., and Li, J. (2019). A High-Efficiency CuO/CeO_2 Catalyst for Diclofenac Degradation in Fenton-Like System. *Front. Chem.* 7, 1–10. doi:10.3389/fchem.2019.00796

Zhu, Y., Zhao, F., Wang, F., Zhou, B., Chen, H., Yuan, R., et al. (2021). Combined the Photocatalysis and Fenton-like Reaction to Efficiently Remove Sulfadiazine in Water Using g-C_3N_4/Ag/γ-FeOOH: Insights Into the Degradation Pathway From Density Functional Theory. *Front. Chem.* 9, 1–15. doi:10.3389/fchem.2021.742459

Conflict of Interest: The authors declare that the research was conducted in the absence of any commercial or financial relationships that could be construed as a potential conflict of interest.

Publisher's Note: All claims expressed in this article are solely those of the authors and do not necessarily represent those of their affiliated organizations, or those of the publisher, the editors, and the reviewers. Any product that may be evaluated in this article, or claim that may be made by its manufacturer, is not guaranteed or endorsed by the publisher.